


<b>TRIUMF - EEC SUBMISSION</b> EEC meeting: 201007S <i>Original Proposal</i>		<b>Exp. No.</b> S1287 - Active (Stage 2)
		<b>Date Submitted:</b> 2010-06-28 23:22:58

---

**Title of Experiment:**

Direct and indirect measurements of the  $^{18}\text{F}(\alpha, p)^{21}\text{Ne}$  reaction with TUDA

---

**Name of group:**

TUDA

---

**Spokesperson(s) for Group**

A.M. Laird, J. Brown

---

**Current Members of Group:**

(name, institution, status, % of research time devoted to experiment)

A.M. Laird	University of York	Lecturer	50%
J. Brown	University of York	Research Associate	50%
J. Fallis	TRIUMF	PDF	15%
A.J. Murphy	University of Edinburgh	Lecturer	10%
B.R. Fulton	University of York	Professor	10%
C. Ruiz	TRIUMF	Research Scientist	10%
C.A. Diget	University of York	Research Associate	10%
F. Herwig	U. of Victoria	Professor	10%
K. Chipps	University of York	Research Associate	10%
L. Buchmann	TRIUMF	Research Scientist	10%
M. Aliotta	University of Edinburgh	Lecturer	10%
M. Pignatari	U. of Victoria/JINA/ TRIUMF	Research Associate	10%

M. Taggart	University of York	Student (PhD)	10%
P. Adsley	University of York	Student (PhD)	10%
S.P. Fox	University of York	Research Associate	10%
T. Davinson	University of Edinburgh	Senior Research	10%
U. Hager	Colorado School of Mines	PDF	10%

---

### **New Beam Requests:**

20 shifts with: TUDA  
*Comment:*

Phase II

19 shifts with: TUDA  
*Comment:*

Phase I

---

### **Basic Information:**

*Date Submitted:* 2010-06-28 23:22:58

*Date Experiment Ready:* 2010-06-29

*Summary:*

Recently, Lee et al. provided the first experimental measurement of the  $^{18}\text{F}(\alpha, p)^{21}\text{Ne}$  reaction rate. This reaction plays an important role in the nucleosynthesis of  $^{19}\text{F}$  and of  $^{21}\text{Ne}$  in low mass stars, in a temperature regime where the experimental measurement still presents large uncertainties. The goal of the present experiment is to measure the  $^{18}\text{F}(\alpha, p)^{21}\text{Ne}$  rate with an independent method with respect to Lee et al., and to reduce the present uncertainty, redefining the present upper limit.

This shall be achieved through cross section measurement of both the direct reaction,  $^{18}\text{F}(\alpha, p)^{21}\text{Ne}$ , and the time-reversed reaction,  $^{21}\text{Ne}(p, \alpha)^{18}\text{F}$ . Both measurements shall be made using the TUDA scattering chamber, using an extended gas target and an array of Si detectors, facilitating coincident measurement of heavy ions and light particles.

Phase one (the direct reaction) shall cover the energy range of  $E_{\text{beam}} = 6.6 - 11 \text{ MeV}$ , equivalent to  $E_{\text{c.m.}} = 1.2 - 2.0 \text{ MeV}$ . This will allow comparison to previous indirect measurements, as well as later normalisation if the time-reversed measurements, in order to account from reactions leading to excited states in  $^{21}\text{Ne}$ .

Phase two (the time-reversed reaction) will cover the energy range  $E_{\text{beam}} = 50.6 - 68.2 \text{ MeV}$ , corresponding to  $E_{\text{c.m.}} = 0.6 - 1.4 \text{ MeV}$  in the  $^{18}\text{F} + \alpha$  system. Cross sections measured for the  $^{21}\text{Ne}(p, a)^{18}\text{F}$  reaction shall be converting into the direct reaction cross sections using the principle of detailed balance, taking into account reactions to excited states in  $^{21}\text{Ne}$ . In all this will provide a continuous cross section measurement from  $E_{\text{c.m.}} = 0.6 - 2.0 \text{ MeV}$ , via methods independent to that used by Lee et al., not only providing a comparison, but also placing tighter constraints on the reaction rates.

Once the new rate with the new uncertainty has been measured, stellar models and the nucleosynthesis codes shall be utilised to evaluate their impact on theoretical stellar yields, specifically  $^{19}\text{F}$  and  $^{21}\text{Ne}$  production in AGB stars.

*Plain Text Summary:* The  $\text{F18}(\alpha, p)\text{Ne21}$  reaction plays an important role in the nucleosynthesis of  $\text{F19}$  and  $\text{Ne21}$  in low mass stars. This experiment will measure this reaction rate, both directly and using the time-reversed reaction,  $\text{Ne21}(p, \alpha)\text{F18}$ . Hydrogen and helium gas target will be used within the TUDA scattering chamber, with an array of silicon detectors for detecting light particles and heavy ions.

*Primary Beam Line:* isac2a

## **ISAC Facilities**

*ISAC Facility:*

*ISAC-I Facility:* TUDA

*ISAC-II Facility:*

## **Secondary Beam**

*Isotope(s):* F18, Ne21

*Energy:* 6.6 - 11 MeV F18. 50.6 -68.2 MeV Ne21

*Energy Units:*

*Energy spread - maximum :*

*Time spread - maximum :*

*Angular Divergence :*

*Spot Size:*

*Intensity Requested:* 1e7 pps F18, 1e8 pps Ne21 pps

*Minimum Intensity:* 5e6 pps F18, 5e7 pps Ne21 pps

*Maximum Intensity:* 1e7 pps F18, 1e8 pps Ne21 pps

*Charge Constraints:*

*Beam Purity:*

*Special Characteristics:*

## **Experiment Support**

*Beam Diagnostics Required:*

*Signals for Beam Tuning:*

*DAQ Support*

*(Summary of Requirements):*

*TRIUMF Support (Resources Needed):*

*NSERC:*

*Other Funding:*

*Safety Issues:*

Safety issues relating to operating TUDA with hydrogen gas will need to be addressed.

*EEC Reader:* 04314

## Direct and indirect measurements of the $^{18}\text{F}(\alpha, p)^{21}\text{Ne}$ reaction with TUDA

### Scientific value of the experiment:

The nucleosynthesis of  $^{19}\text{F}$  in the galaxy still remains an open puzzle in stellar astrophysics. Several astrophysical sources have been proposed so far, among them neutrino spallation on  $^{20}\text{Ne}$  during supernova explosions of massive stars (SNII, e.g. [1, 2]), in low mass Asymptotic Giant Branch (AGB) stars during the convective thermal pulse (TP) (e.g. [3, 4, 5]), and in the winds of Wolf-Rayet stars [6, 7]. In particular, in AGB stars the main reaction flow producing fluorine is  $^{14}\text{N}(\alpha, \gamma)^{18}\text{F}(\beta^+)^{18}\text{O}(\text{p}, \alpha)^{15}\text{N}(\alpha, \gamma)^{19}\text{F}$  at  $\sim 20\text{-}30$  keV, where protons in the He rich He inter-shell during the TP are provided by the  $^{14}\text{N}(\text{n}, \text{p})^{14}\text{C}$  reaction, neutrons by the  $^{13}\text{C}(\alpha, \text{n})^{16}\text{O}$  reaction, whilst  $^{14}\text{N}$  and  $^{13}\text{C}$  are present in the ashes of the H shell [3]. For other secondary processes producing fluorine in AGB stars see for example [8, 9, 4]. Although massive stars could theoretically reproduce all the solar  $^{19}\text{F}$  abundances within the uncertainties of the neutrino rates (e.g. [2]), AGB stars are the only astrophysical objects where a strong production of  $^{19}\text{F}$  has been observed, both in AGB stars (see [3, 5] for AGB stars at solar metallicity, [10] and [11] for AGB stars at low metallicity), in post-AGB stars (e.g. [12]) and in planetary nebulae (e.g. [13]), whereas no clear observational evidence have been found for a strong  $^{19}\text{F}$  production in SNII [14].

Driven by the new  $^{18}\text{F}(\alpha, \text{p})^{21}\text{Ne}$  experimental measurement by Lee et al. [15], Karakas et al. [16] analyzed the impact of this reaction on  $^{19}\text{F}$  production in AGB stars. At the stellar energies of interest (20-30 keV), the upper limit of the  $^{18}\text{F}(\alpha, \text{p})^{21}\text{Ne}$  rate is 2 orders of magnitude or more higher than the recommended rate. Using the upper limit rate, the  $^{18}\text{F}(\alpha, \text{p})^{21}\text{Ne}$  competes more efficiently with the  $^{18}\text{F}(\beta^+)^{18}\text{O}$  process, reducing the amount of  $^{18}\text{O}$ , but providing more protons to be captured by  $^{18}\text{O}$ . According to Karakas et al. [16], therefore, the upper limit of  $^{18}\text{F}(\alpha, \text{p})^{21}\text{Ne}$  causes a more significant production of  $^{19}\text{F}$  via  $^{18}\text{O}(\text{p}, \alpha)^{15}\text{N}(\alpha, \gamma)^{19}\text{F}$ , with respect to using the recommended rate of  $^{18}\text{F}(\alpha, \text{p})^{21}\text{Ne}$  (see Fig. 1).

For this reason, the main goal of the present proposal is to reduce the present uncertainty of the  $^{18}\text{F}(\alpha, \text{p})^{21}\text{Ne}$  rate at temperature of  $\sim 0.3$  GK, in particular improving the reliability of the present upper limit of this rate (see Fig. 2).

The upper limit rate of the  $^{18}\text{F}(\alpha, \text{p})^{21}\text{Ne}$  reaction rate would also imply an increased  $^{21}\text{Ne}$  production in the He inter-shell in AGB stars, affecting the Ne isotopic ratios [16]. Ne abundances are measured in mainstream SiC presolar grains, that have been condensed in the envelope of low mass AGB stars and that carry the signature of the parent stars (e.g. [17]). In particular, the  $^{21}\text{Ne}/^{22}\text{Ne}$  ratio that is measured over a large sample of grains (e.g. [18]) and single SiC grains (e.g. [19]), is significantly larger than what is predicted by theoretical stellar models (e.g. [20, 18, 16]). As a possible source of the extra  $^{21}\text{Ne}$ , Lewis et al. [18] proposed spallation due to interaction with cosmic rays when the grain is exposed in the interstellar medium. Ott and Begemann [21] argued against this possibility, pointing to a stellar nucleosynthesis origin of  $^{21}\text{Ne}$ . Indeed, Karakas [16] showed that using the upper limit of the  $^{18}\text{F}(\alpha, \text{p})^{21}\text{Ne}$  rate, the  $^{21}\text{Ne}/^{22}\text{Ne}$  ratio observed in presolar SiC grains may be reproduced in stellar AGB models (see Fig. 3). Therefore, in order to confirm the cosmogenic or stellar nucleosynthetic origin of  $^{21}\text{Ne}$  in presolar SiC grains, a more precise measurement of the  $^{18}\text{F}(\alpha, \text{p})^{21}\text{Ne}$  rate is required.

The previous measurements by Lee et al. [15, 22] used the time-reversed reaction, in conjunction with the activation method, to determine cross sections for the  $^{18}\text{F}(\alpha, \text{p})^{21}\text{Ne}$  reaction.  $^{21}\text{Ne}$  was implanted into Cu/Au targets, which were subsequently bombarded with protons at a series of different energies, for two half-lives of  $^{18}\text{F}$ . The 511 keV annihilation radiation produced following the  $\beta^+$  decay of  $^{18}\text{F}$ , was then counted off-line using two HPGe detectors in coincidence mode.

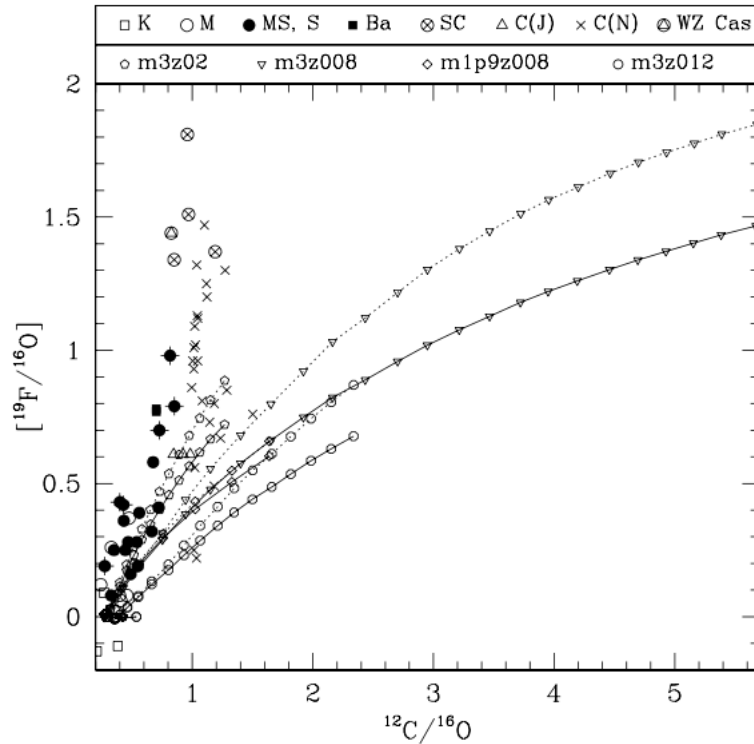


Figure 1: Reproduced from Figure 3 of [16]: “Comparison of fluorine abundances observed by Jorissen et al. (1992) and model predictions for selected stellar models:  $3 M_{\odot}$  with  $Z = 0.02, 0.012,$  and  $0.008$ ; and  $1.9 M_{\odot}$  with  $Z = 0.008$ . All models include a PMZ [partial mixing zone] of  $0.002 M_{\odot}$ . Predictions are normalized in such way that the initial  $^{19}\text{F}$  abundance corresponds to the average F abundance observed in K and M stars (see Jorissen et al. 1992). Crossed MS and S symbols denote stars with large N excesses. Each symbol on the prediction lines represents a TDU [third dredge-up] episode. *Solid lines*: Calculations performed using no  $^{18}\text{F}(\alpha, p)^{21}\text{Ne}$  reaction, which are equivalent to using the current lower limit, recommended value and Brussels library rate. *Dotted lines*: Calculations performed using the current upper limit of the rate.”

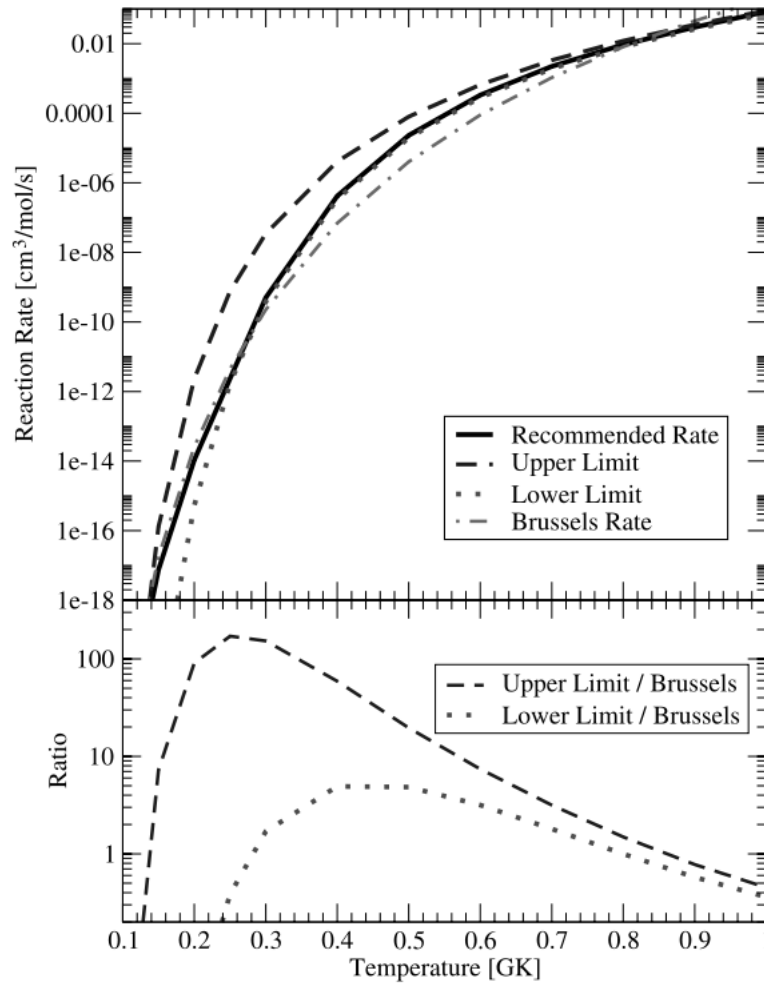


Figure 2: Reproduced from Figure 1 of [16]: “Reaction rate of  $^{18}\text{F}(\alpha, p)^{21}\text{Ne}$  including the upper and lower limits. Also shown is the Brussels theoretical estimate of this rate. In the bottom panel, the ratios of the current upper and lower limits with respect to the Brussels rate are shown.”

Oxygen contamination on the backing material produced a background rate due to the  $^{18}\text{O}(p, n)^{18}\text{F}$  and  $^{17}\text{O}(p, \gamma)^{18}\text{F}$  reactions, despite considerable efforts to minimise this contamination. Although Lee et al. made attempts to account for this background in their analysis, the introduced of a systematic error is inevitable, thus making the case for confirmation of the cross sections via an independent technique.

Furthermore, the  $^{18}\text{F}(\alpha, p)^{21}\text{Ne}$  reaction is known to produce  $^{21}\text{Ne}$  in several excited states, as well as its ground state (see Fig. 4 for a level scheme of low-lying states in  $^{21}\text{Ne}$ ). The time-reversed reaction is not sensitive to this part of the cross section, therefore a measurement of the direct reaction process is required.

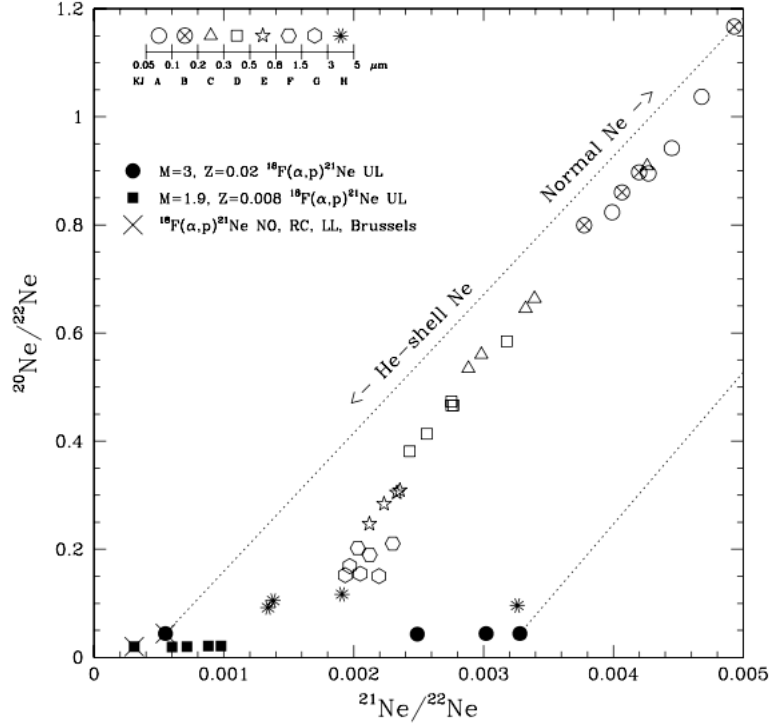


Figure 3: Reproduced from Figure 2 of [16]: “Ne isotopic ratios observed in meteoritic SiC grains and predicted in the inter-shell of our  $3 M_{\odot}$ ,  $Z = 0.02$  and  $1.9 M_{\odot}$ ,  $Z = 0.008$  models. The plot is similar to Fig. 8 of Lewis et al. (1994), where we have taken their measurements and added the model predictions. For each model we plot the Ne isotopic ratios in the He inter-shell at the end of each TP occurring when  $\text{C}/\text{O} > 1$  is satisfied in the envelope of the star. The crossed filled symbols represent models computed without the  $^{18}\text{F}(\alpha, p)^{21}\text{Ne}$  reaction rate, which give a constant result. The filled symbols represent models run using the upper limit of the  $^{18}\text{F}(\alpha, p)^{21}\text{Ne}$  reaction rate. Dotted lines connect the normal Ne component of solar composition to the He-shell Ne component corresponding to the final compositions of the inter-shell for the  $3 M_{\odot}$ ,  $Z = 0.02$  model.”

### Description of the experiment:

We propose to measure the  $^{18}\text{F}(\alpha, p)^{21}\text{Ne}$  reaction rate via two complementary methods, i.e. through the direct reaction, and using the time-reversed reaction,  $^{21}\text{Ne}(p, \alpha)^{18}\text{F}$ .

Measurements of the direct reaction have previously proved difficult [15], indeed, no results from previous attempts have ever been formally published. This is, in part, due to the lack of intense



$^{18}\text{F}$  beams, and the difficulty in producing a suitably thick  $^4\text{He}$  target. We propose to measure the direct reaction only at relatively high energies, utilising the intense  $^{18}\text{F}$  beams now available at TRIUMF and an extended gas target. The energy range covered shall be chosen such that it overlaps with previous indirect measurements, allowing an independent comparison with different systematic errors. A radioactive  $^{18}\text{F}$  beam shall be utilised with this experimental set-up to measure the direct reaction rate for centre-of-mass energies from  $E_{c.m.} = 1.2$  to 2.0 MeV in 200 keV steps, corresponding to beam energies of 6.6 to 11 MeV. Using a gas pressure of 50 Torr produces energy loss through the target of 200 keV in the centre-of-mass, thus giving a continuous measurement across this energy range.

For the lowest energies of interest, the  $^{18}\text{F}(\alpha, p)^{21}\text{Ne}$  reaction rate becomes too low to be measured via the direct reaction within a reasonable time frame. The time-reversed reaction shall therefore be employed. The kinematics of the time-reversed reaction result in highly forward focused reaction products. This effect is so severe that use of a conventional  $\text{CH}_2$  target prohibits the use of the beam intensities required to measure the energy region of interest due to the high rate from Rutherford scattering at similar angles to the reaction products. For this reason, a similar approach to that described above for the direct reaction shall be employed, i.e. the TUDA scattering chamber will be filled with hydrogen gas, and a similar arrangement of detectors utilised. This system has the added advantage that the beam energy loss through the target is no longer dominated by the presence of the carbon, thus an effectively thicker target may be utilised for the same energy “bite”. Furthermore, any background resulting from reactions with the carbon is eliminated. A stable beam of  $^{21}\text{Ne}$  with energies ranging from 50.6 to 68.2 MeV shall be utilised, corresponding to energies of 0.6 to 1.4 MeV in the  $^{18}\text{F} + \alpha$  system, in steps of 200 keV. Once again, by choosing a target pressure of 250 Torr, an energy loss of  $\sim 200$  keV across the target is achieved, allowing complete measurement of the cross section across the energy range.

As stated previously, the time-reversed reaction is not sensitive to reactions proceeding through anything but the ground state of  $^{21}\text{Ne}$ . Furthermore, it is thought that the ratio of transitions to different final states in  $^{21}\text{Ne}$  will vary as a function of energy. It is therefore crucial that we determine this for a variety of energies in the direct reaction, such that we can understand the effects this will play at lower energies and normalise the cross sections to account for these additional states. Again, the energy range of the time-reversed reaction measurement shall be chosen such that it overlaps with that measured directly, but shall extend to considerably lower energies within the Gamow window (420 - 700 keV) for the astrophysical environment of interest.

The extracted cross section from this measurement can be readily converted into the corresponding direct reaction cross section using the principle of detailed balanced, and taking into account the ratios of reactions going to the ground state versus excited states, determined using the direct reaction approach.

### **Experimental equipment:**

Measurement shall be achieved using silicon strip detector arrays and a gas target within the TUDA scattering chamber. A significant hurdle in experiments such as this is the detection of the heavy ions. These ions are typically stopped in the exit window of the gas target. In order to overcome this, rather than using a gas cell, the TUDA chamber will be filled with gas, contained by a thin entrance window (e.g 2  $\mu\text{m}$  Ni) placed on a re-entrant flange (see Fig. 5). This arrangement will allow for coincident detection of both heavy ions and light reaction products, hence the reactions of interest can be extracted with minimal contribution from background events. Scattering from the entrance window will be monitored with photodiodes to provide beam normalisation.

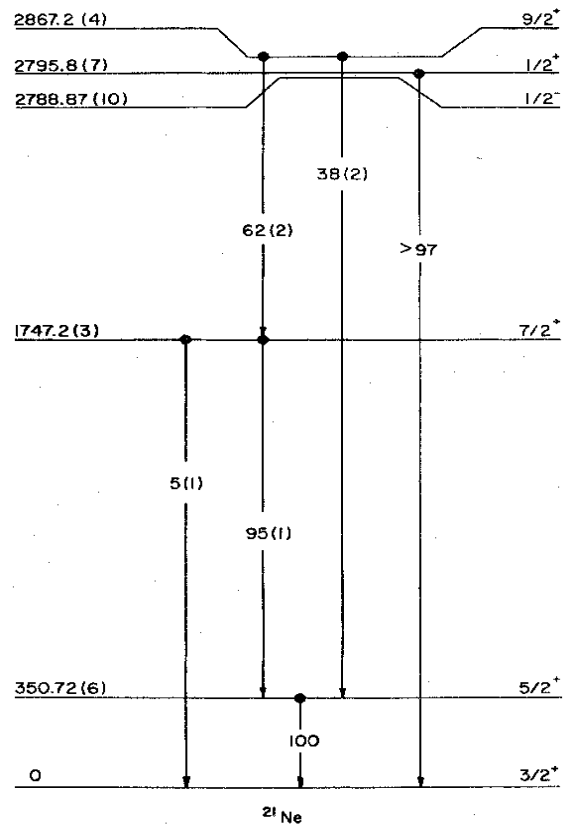


Figure 4: Energy level scheme of low-lying states in  $^{21}\text{Ne}$ .

For the direct reaction measurement, the  $^{18}\text{O}(\alpha, p)^{21}\text{F}$  reaction channel (resulting from any  $^{18}\text{O}$  contamination in the beam) is not open in this energy range (although oxygen contamination within the beam can be minimised by flushing the source with xenon). The largest potential source of background is therefore thought to be protons scattered from water vapour deposited on the entrance window of the chamber. This can be minimised by use of an anti-scatter shield between the window and the upstream CD detectors. A similar shield will be placed downstream of the second set of CD detectors to shield them from reactions taking place between this and the third CD detector arrangement.

The requirement for coincident detection of particles and heavy ions should virtually eliminate any remaining background events. Additionally, coincidence events will be confirmed by requiring co-planarity and  $ToF$  difference conditions. Furthermore, at the energies suggested, contributions from possible fusion reactions with the entrance window are expected to be minimal. Nevertheless, such effects shall be determined using background runs taken without gas in the chamber.

The silicon array will consist of a box of W-type DSSSDs, with an upstream CD detector and downstream CD  $\Delta E - E$  telescope, for the detection protons and  $\alpha$  particles. A additional CD  $\Delta E - E$  telescope placed further downstream will allow the detection of the heavy ions. A schematic diagram of the proposed set-up is shown in Fig. 5.

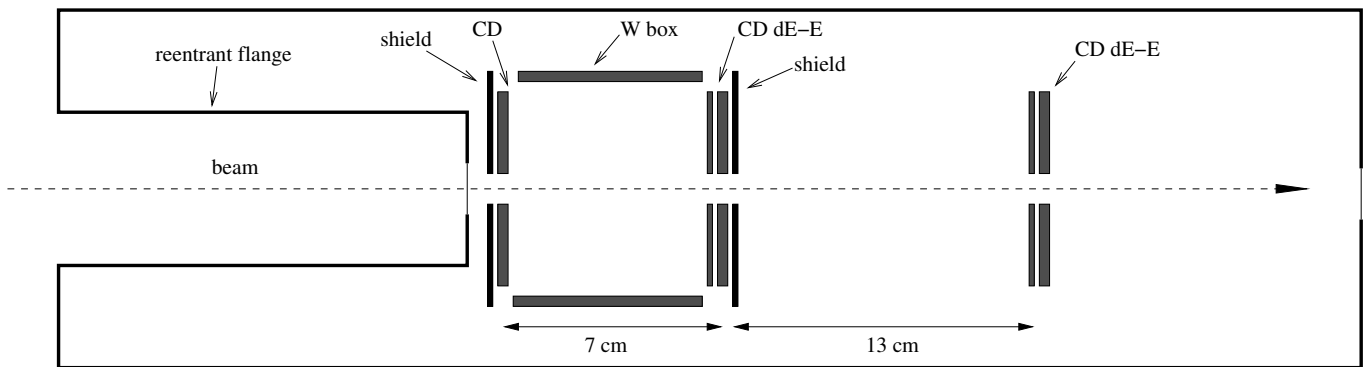


Figure 5: Schematic diagram of the proposed detector arrangement for the direct beam measurement (not to scale). The TUDA chamber is filled with He gas, contained by a thin entrance window mounted on a re-entrant flange. Detectors positions are indicated, though these may be varied in order to optimise angular coverage. The anti-scattering shields and re-entrant flange are indicated, photodiodes for beam normalisation are not shown. See text for details.

### Readiness:

The TUDA scattering chamber and all detectors and electronics are available for both measurements proposed. Fabrication of the necessary structural components is expected to be completed well in advance of any likely running date. Safety aspects related to operating TUDA with  $\text{H}_2$  gas will need to be addressed.

All beams requested for the experiment are currently available at the required intensities, we therefore request stage two approval.

### Beam time required:

The experiment shall be split into two phases: phase 1 shall measure the direct reaction at high energies, phase 2 shall measure the time-reversed reaction at low energies. These phases do not need to be run consecutively, and can take place in either order. We request a total of 19 shifts for phase 1, including 4.5 shifts for beam energy changes and 3.5 shifts for background runs without gas in the chamber. For phase 2, we require 20 shifts, including 4.5 shifts for beam tuning and 3.5 for background runs without the target. See Table 1 for detailed breakdown.

Table 1: Breakdown of shifts requested and expected yields.

	$E_{lab}$ MeV	$E_{c.m}$ MeV	$E_{c.m}(\text{direct})$ MeV	$\sigma$ mb	Yield counts/hr	Shifts 12 hrs	Total Counts
Phase 1	11	2.0	2.0	10	1750	0.5	10500
	9.9	1.8	1.8	1.0	214	0.5	1284
	8.8	1.6	1.6	$2.0 \times 10^{-1}$	38	1	456
	7.7	1.4	1.4	$3.3 \times 10^{-2}$	6.7	2	160.8
	6.6	1.2	1.2	$6.0 \times 10^{-3}$	1.2	7	100.8
Phase 2	68.2	3.1	1.4	$7.7 \times 10^{-2}$	1500	0.5	18000
	63.8	2.9	1.2	$1.3 \times 10^{-2}$	260	0.5	3120
	59.4	2.7	1.0	$2.1 \times 10^{-3}$	43	1	1030
	55.0	2.5	0.8	$3.5 \times 10^{-4}$	7.1	2	170
	50.6	2.3	0.6	$5.8 \times 10^{-5}$	1.2	8	113

This request is based on yields calculated as  $Y = \sigma N_b N_t \eta$ , with the following assumptions:

- $N_b = 1 \times 10^7$  pps  $^{18}\text{F}$  and  $1 \times 10^8$  pps  $^{21}\text{Ne}$ , for the direct and reverse reaction respectively,
- $N_t(\text{direct}) \sim 1 \times 10^{19}$   $^4\text{He}/\text{cm}^2$ , based on a pressure of 50 Torr and an active target region of  $\sim 7$  cm,
- $N_t(\text{reverse}) \sim 1 \times 10^{20}$   $p/\text{cm}^2$ , based on a pressure of 250 Torr and an active target region of  $\sim 7$  cm,
- conservative estimate of detection efficiency,  $\eta \sim 50\%$ ,
- cross sections for the  $^{21}\text{Ne}(p, \alpha)^{18}\text{F}$  reaction have been extracted from Fig. 4 of [22] (see Fig. 6), and extrapolated to lower energies,
- cross sections for the  $^{18}\text{F}(\alpha, p)^{21}\text{Ne}$  reaction have been calculated from the above using the principle of detailed balance.

### Data analysis:

To be done with existing TUDA analysis packages, no Triumf support will be required.

Once the new rate with the new uncertainty has been measured, Falk Herwig and Marco Pignatari (members of the team submitting this proposal) will provide the stellar models and the nucleosynthesis codes to evaluate their impact on theoretical stellar yields, specifically  $^{19}\text{F}$  and  $^{21}\text{Ne}$  production in AGB stars.

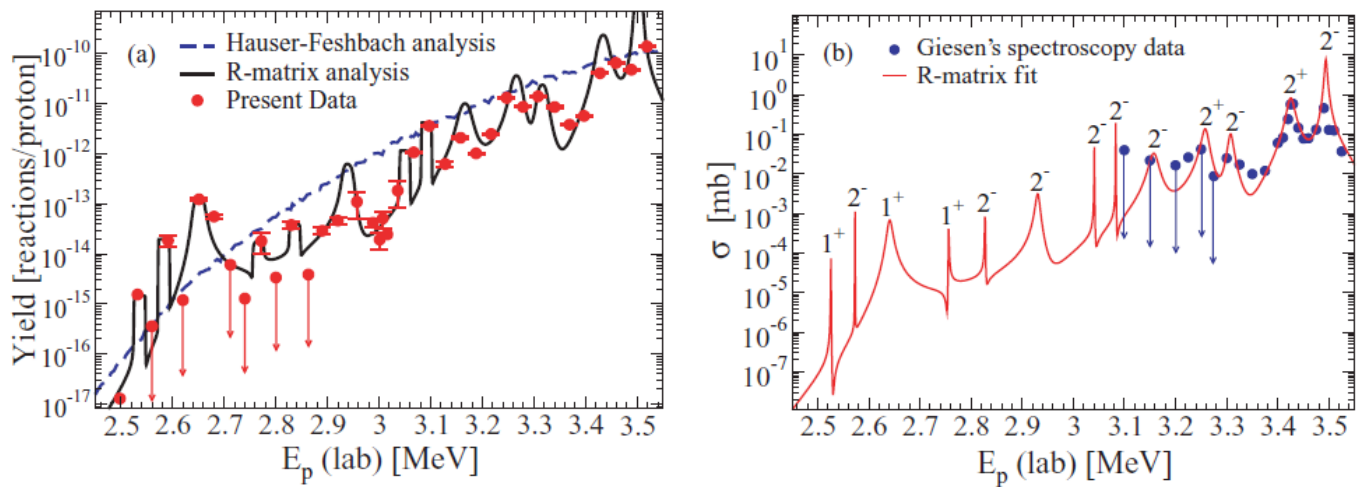


Figure 6: Reproduced from Figure 4 of [22]: “Panel (a) shows comparison between the present experimental yields and the yield prediction from Hauser-Feshbach calculations (dashed line) and the calculations based on an  $R$ -matrix fit to the data (solid line). Panel (b) shows the  $R$ -matrix cross section, which is obtained by fitting to the previous spectroscopy data [14] as described in the text.”

## References:

- [1] S. E. Woosley and W. C. Haxton. Supernova neutrinos, neutral currents and the origin of fluorine. *Nature*, 334(6177):45–47, July 1988.
- [2] S. E. Woosley and T. A. Weaver. The evolution and explosion of massive stars. II. Explosive hydrodynamics and nucleosynthesis. *Astrophysical Journal Supplement*, 101:181–+, November 1995.
- [3] A. Jorissen, V. V. Smith, and D. L. Lambert. Fluorine in red giant stars - evidence for nucleosynthesis. *Astronomy and Astrophysics*, 261:164–187, July 1992.
- [4] S. Cristallo, O. Straniero, R. Gallino, L. Piersanti, I. Domnguez, and M. T. Lederer. Evolution, nucleosynthesis, and yields of low-mass asymptotic giant branch stars at different metallicities. *The Astrophysical Journal*, 696(1):797, 2009.
- [5] C. Abia, K. Cunha, S. Cristallo, P. de Laverny, I. Domnguez, K. Eriksson, L. Gialanella, K. Hinkle, G. Imbriani, A. Recio-Blanco, V. V. Smith, O. Straniero, and R. Wahlin. Fluorine abundances in galactic asymptotic giant branch stars. *The Astrophysical Journal Letters*, 715(2):L94, 2010.
- [6] G. Meynet and M. Arnould. Synthesis of  $^{19}\text{F}$  in Wolf-Rayet stars. *Astronomy and Astrophysics*, 355:176–180, March 2000.
- [7] A. Palacios, M. Arnould, and G. Meynet. The thermonuclear production of  $^{19}\text{F}$  by Wolf-Rayet stars revisited. *A&A*, 443(1):243–250, November 2005.
- [8] S. Goriely and N. Mowlavi. Neutron-capture nucleosynthesis in AGB stars. *Astronomy and Astrophysics*, 362:599–614, October 2000.
- [9] Maria Lugaro, Claudio Ugalde, Amanda I. Karakas, Joachim Gress, Michael Wiescher, John C. Lattanzio, and Robert C. Cannon. Reaction rate uncertainties and the production of  $^{19}\text{F}$  in asymptotic giant branch stars. *The Astrophysical Journal*, 615(2):934, 2004.
- [10] Simon C. Schuler, Katia Cunha, Verne V. Smith, Thirupathi Sivarani, Timothy C. Beers, and Young Sun Lee. Fluorine in a carbon-enhanced metal-poor star. *The Astrophysical Journal Letters*, 667(1):L81, 2007.

- [11] S. Lucatello, T. Masseron, and J. A. Johnson. Carbon-enhanced, metal-poor stars and modeling of the asymptotic giant branch. *Publications of the Astronomical Society of Australia*, 26:303–310, September 2009.
- [12] K. Werner, T. Rauch, and J. W. Kruk. Fluorine in extremely hot post-AGB stars: Evidence for nucleosynthesis. *A&A*, 433(2):641–645, April 2005.
- [13] Masaaki Otsuka, Hideyuki Izumiura, Akito Tajitsu, and Siek Hyung. Detection of fluorine in the halo planetary nebula BoBn 1: Evidence for a binary progenitor star. *The Astrophysical Journal Letters*, 682(2):L105, 2008.
- [14] S. R. Federman, Yaron Sheffer, David L. Lambert, and V. V. Smith. Far ultraviolet spectroscopic explorer measurements of interstellar fluorine. *The Astrophysical Journal*, 619(2):884, 2005.
- [15] H.Y. Lee et al.  $^{18}\text{F}(\alpha, p)^{21}\text{Ne}$  as an alternative neutron source for the r-process in Supernovae. *10th Symposium on Nuclei in the Cosmos*, 2006.
- [16] Amanda I. Karakas, Hye Young Lee, Maria Lugaro, J. Görres, and M. Wiescher. The impact of the  $^{18}\text{F}(\alpha, p)^{21}\text{Ne}$  reaction on asymptotic giant branch nucleosynthesis. *The Astrophysical Journal*, 676(2):1254–1261, 2008.
- [17] Ernst Zinner, Sachiko Amari, Robert Guinness, Cristine Jennings, Aaron F. Mertz, Ann N. Nguyen, Roberto Gallino, Peter Hoppe, Maria Lugaro, Larry R. Nittler, and Roy S. Lewis. NanoSIMS isotopic analysis of small presolar grains: Search for  $\text{Si}_3\text{N}_4$  grains from AGB stars and Al and Ti isotopic compositions of rare presolar SiC grains. *Geochimica et Cosmochimica Acta*, 71(19):4786–4813, October 2007.
- [18] Roy S Lewis, Sachiko Amari, and Edward Anders. Interstellar grains in meteorites: II. SiC and its noble gases. *Geochimica et Cosmochimica Acta*, 58(1):471–494, January 1994.
- [19] Philipp R. Heck, Kuljeet K. Marhas, Peter Hoppe, Roberto Gallino, Heinrich Baur, and Rainer Wieler. Presolar He and Ne isotopes in single circumstellar SiC grains. *The Astrophysical Journal*, 656(2):1208, 2007.
- [20] R. Gallino, M. Busso, G. Picchio, and C. M. Raiteri. On the astrophysical interpretation of isotope anomalies in meteoritic SiC grains. *Nature*, 348:298–302, November 1990.
- [21] U. Ott and F. Begemann. Spallation recoil and age of presolar grains in meteorites. *Meteoritics and Planetary Science*, 35:53–63, January 2000.
- [22] H. Y. Lee, M. Couder, A. Couture, S. Falahat, J. Grres, L. Lamm, P. J. LeBlanc, S. O’Brien, A. Palumbo, E. Stech, E. Strandberg, W. Tan, C. Ugalde, and M. Wiescher. Cross-section measurement of the  $^{18}\text{F}(\alpha, p)^{21}\text{Ne}$  reaction and possible implication for neutron production in explosive helium burning. *Phys. Rev. C*, 80(2):025805–, August 2009.